
Learning to Teach with Deep Interactions*

¹Yang Fan, ²Yingce Xia, ²Lijun Wu, ²Shufang Xie, ²Weiqing Liu,
²Jiang Bian, ²Tao Qin, ¹Xiang-Yang Li, ²Tie-Yan Liu

¹ University of Science and Technology of China ² Microsoft Research Asia

¹fyabc@mail.ustc.edu.cn, xiangyangli@ustc.edu.cn

²{yingce.xia,lijun.wu,shufxi,weiqing.liu,jiang.bian,taoqin,tyliu}@microsoft.com

Abstract

Machine teaching [42, 37] uses a meta/teacher model to guide the training of a student model (which will be used in real tasks) through training data selection, loss function design, etc. Previously, the teacher model only takes shallow/surface information as inputs (e.g., training iteration number, loss and accuracy from training/validation sets) while ignoring the internal states of the student model, which limits the potential of learning to teach. In this work, we propose an improved data teaching algorithm, where the teacher model deeply interacts with the student model by accessing its internal states. The teacher model is jointly trained with the student model using meta gradients propagated from a validation set. We conduct experiments on image classification with clean/noisy labels and empirically demonstrate that our algorithm makes significant improvement over previous data teaching methods.

1 Introduction

In recent years, machine teaching [42, 20, 21], also known as learning to teach [6, 37], has become a popular topic in deep learning. Learning to teach is a meta-learning paradigm that involves a teacher model and a student model. The student model is our final target and used for real tasks, like image classification [12], objection detection [30], etc., while the teacher model is used to guide the training of the student model through adjusting the weights of training data [6, 34, 14, 29], generating better loss functions [37], etc. These approaches have demonstrated promising results in image classification (with both clean and noisy labels) [14, 34], machine translation [37], and text classification [6].

Previously, the teacher model only utilizes surface information derived from the student model. In [6, 37, 34, 14], the inputs of the teacher model include training iteration number, training loss (as well as the margin [32]), validation loss, the output of the student model, etc. In those algorithms, the teacher model does not leverage the internal states of the student model, e.g., the values of the second-to-last layer and even deeper layers far from the output layer of a neural network based student model. We notice that the internal states of a model have been widely investigated and shown its effectiveness in many deep learning algorithms and tasks. In ELMo [26], a pre-trained LSTM provides its internal states, the values of each layer, for downstream tasks as feature representations. In image captioning tasks [38, 2], a faster RCNN [30] pre-trained on ImageNet provides its internal states (i.e., mean-pooled convolutional features) of the selected regions, serving as representations of images [2]. In knowledge distillation [31, 1], a student model mimics the output of the internal layers of the teacher model so as to achieve comparable performances with the teacher model. Unfortunately, this kind of deep information is missing in learning to teach algorithms. The success of leveraging internal states in the above applications motivates us to investigate them in learning to teach, which leads to deep interactions between the teacher and student model.

*This work is conducted at Microsoft Research Asia.

We propose a new data teaching algorithm, where the teacher model and the student model have deep interactions: the student model provides its internal states (i.e., the values of its second-to-last layer) and optionally values of its output layer which serve as the inputs of the teacher model, and the teacher model outputs adaptive weights of training samples which are used to enhance the training of the student model. Figure 1 illustrates the key difference between our algorithm (the right figure) and previous data teaching algorithm [6, 37] (the left figure). We decompose the student model into a feature extractor, which can process the input x to an internal state c , and a classifier (denoted as “cls”), which is a relatively shallow model like a linear classifier to map c to the final prediction \hat{y} . In previous data teaching algorithm, the teacher model only takes the surface information of the student model as inputs like training and validation loss, which are related to \hat{y} and ground truth label y but not explicitly related to the internal states c . In contrast, the teacher model in our algorithm leverages both the final outputs \hat{y} and the internal states c of the student model as inputs. In this way, more information from the student model is accessible. In our algorithm, the teacher and the student models are jointly optimized in an alternative way, where the teacher model is updated according to the validation signal via reverse-mode differentiation [23], and the student model tries to minimize the loss on weighted data. Experimental results on CIFAR-10 and CIFAR-100 [17] with both clean labels and noisy labels demonstrate the effectiveness of our algorithm. We achieve promising results over previous methods of learning to teach.

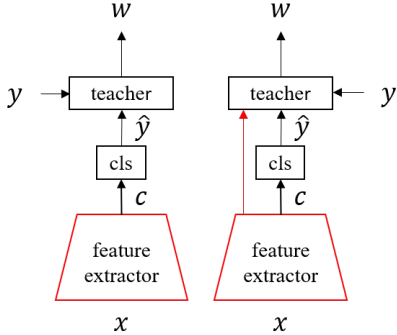


Figure 1: Comparison between the previous teacher model [6] (left) and ours (right).

The remaining part is organized as follows. Related work is discussed in Section 2. Our algorithm is introduced in Section 3. The experiments with clean labels and noisy labels are reported in Section 4 and Section 5 respectively. Section 6 concludes this paper and discusses future directions.

2 Related work

Assigning weights to different data points have been widely investigated in literature, where the weights can be either continuous [8, 14] or binary [6, 4]. The weights can be explicitly bundled with data, like Boosting and AdaBoost methods [7, 11, 8] where the weights of incorrectly classified data are gradually increased, or implicitly achieved by controlling the sampling probability, like hard negative mining [24] where the harder examples in a previous round will be sampled again in the next round. As a comparison, in self-paced learning (SPL) [18], weights of hard examples will be assigned to zero in the early stage of training, and the threshold is gradually increased during the training process to control the student model to learn from easy to hard. An important motivation of data weighting is to increase the robustness of training, including addressing the problem of imbalanced data [36, 5, 15], biased data [39, 29], noisy data [3, 28, 35, 16].

Except for manually designing weights for the data, there is another branch of work that leverages a meta model to assign weights. Learning to teach [6] is a learning paradigm where there is a student model for the real task, and a teacher model to guide the training of the student model. Based on the collected information, the teacher model provides signals to the student model, which can be the weights of training data [6], adaptive loss functions [37], etc. The general scheme of machine teaching is discussed and summarized in [42]. The concept of teaching can be found in label propagation [9, 10], pedagogical teaching [13, 33], etc. [21] leverages a teaching way to speed up the training, where the teacher model selects the training data balancing the trade off between the difficulty and usefulness of the data. [34, 29, 14] mainly focuses on the setting that the data is biased or imbalanced. According to our knowledge, our work is the first one that the teacher and student can deeply interact. In previous work, the teacher model only access the surface information of the student model, while our teacher model can access the internal states of the student model. We will empirically verify the benefits of our proposals.

3 Our method

We focus on data teaching in this work, where the teacher model assigns an adaptive weight to each sample. We first introduce the notations used in this work, then describe our algorithm, and finally provide some discussions.

3.1 Notations

Let \mathcal{X} and \mathcal{Y} denote the source domain and the target domain respectively. We want to learn a mapping f , i.e., the student model, from \mathcal{X} and \mathcal{Y} . W.l.o.g, we can decompose f into a feature extractor and a decision maker, denoted as φ_f and φ_d respectively, where $\varphi_f : \mathcal{X} \mapsto \mathbb{R}^d$, $\varphi_d : \mathbb{R}^d \mapsto \mathcal{Y}$, and d is the dimension of the extracted feature. That is, for any $x \in \mathcal{X}$, $f(x) = \varphi_d(\varphi_f(x))$. We denote the parameters of f as θ . In our work, we mainly work on the image classification problem. Given a classification network f , the default segmentation method is that $\varphi_f(\cdot)$ is the output of the second-to-last layer, and φ_d is a linear classifier taking $\varphi_f(x)$ as input.

Let $\phi(I, M; \omega)$ denote the teacher model parameterized by ω , where I is the internal states of a student model and M is the surface information like training iteration, training loss, labels of the samples, etc. ϕ can map an input sample $(x, y) \in \mathcal{X} \times \mathcal{Y}$ to a non-negative scalar, representing the weight of the sample. Let $\ell(f(x), y; \theta)$ denote the training loss on sample pair (x, y) , and $R(\theta)$ is a regularization term on θ , independent of the training samples.

Let D_{train} and D_{valid} denote the training and validation sets respectively, both of which are subsets of $\mathcal{X} \times \mathcal{Y}$ with N_T and N_V samples. Denote the validation metric as $m(y, \hat{y})$, where y and \hat{y} are the ground truth label and predicted label respectively. We require that $m(\cdot, \cdot)$ should be a differentiable function w.r.t. the second input. $m(y, \hat{y})$ can be specialized as the expected accuracy [37] or the log-likelihood on the validation set. Define $M(D_{\text{valid}}; \theta)$ as $\frac{1}{N_V} \sum_{(x,y) \in D_{\text{valid}}} m(y, f(x; \theta))$.

3.2 Algorithm

The teacher model outputs a weight for any input data. When facing a real-world machine learning problem, we need to fit a student model on the training data, select the best model according to validation performance, and apply it to the test set. Since the test set is not accessible during training and model selection, we need to maximize the validation performance of the student model. This can be formulated as a bi-level optimization problem:

$$\begin{aligned} & \max_{\omega, \theta^*(\omega)} M(D_{\text{valid}}; \theta^*(\omega)) \\ \text{s.t. } & \theta^*(\omega) = \underset{\theta}{\operatorname{argmin}} \frac{1}{N_T} \sum_{i=1}^{N_T} w(x_i, y_i) \ell(f(x_i), y_i; \theta) + \lambda R(\theta), \\ & w(x_i, y_i) = \phi(\varphi_f(x_i), M; \omega), \end{aligned} \quad (1)$$

where λ is a hyperparameter, and $w(x_i)$ represents the weight of data x_i . The task of the student model is to minimize the loss on weighted data, as shown in the second line of Eqn.(1). Without a teacher, all $w(x_i)$'s are fixed as one. In a learning-to-teach framework, the parameters of the teacher model (i.e., ω) and the student model (i.e., θ) are jointly optimized. Eqn.(1) is optimized in an iterative way, where we calculate $\theta^*(\omega)$ based on a given ω , then we update ω based on the obtained $\theta^*(\omega)$. We need to figure out how to obtain θ^* , and how to calculate $\frac{\partial}{\partial \omega} M(D_{\text{valid}}; \theta^*(\omega))$.

Obtaining $\theta^*(\omega)$: Considering a deep neural network is highly non-convex, generally, we are not able to get the closed-form solution of the θ^* in Eqn.(1). We choose stochastic gradient descend method (briefly, SGD) with momentum for optimization [27], which is an iterative algorithm. We use a subscript t to denote the t -th step in optimization. D_t is the data of the t -th minibatch, with the k -th sample $(x_{t,k}, y_{t,k})$ in it. For ease of reference, denote w_t as a column vector, where the k -th element is the weight for sample $(x_{t,k}, y_{t,k})$, and $\ell(D_t; \theta_t)$ is another column vector with the k -element $\ell(f(x_{t,k}), y_{t,k}; \theta_t)$, both of which are defined in Eqn.(1). Following the implementation of PyTorch [25], the update rule of momentum SGD is:

$$v_{t+1} = \mu v_t + \frac{\partial}{\partial \theta_t} \left[\frac{1}{|D_t|} w_t^\top \ell(D_t; \theta_t) + \lambda R(\theta_t) \right]; \quad \theta_{t+1} = \theta_t - \eta_t v_{t+1}, \quad (2)$$

where $\theta_0 = v_0 = 0$. η_t is the learning rate at the t -th step, and μ is the momentum coefficient. Assume we update the model for K steps. We can eventually obtain θ_K , which serves as the proxy for θ^* . To stabilize the training, we will set $\frac{\partial w_t}{\partial \theta_t} = 0$.

Calculating $\frac{\partial}{\partial \omega} M(D_{\text{valid}}; \theta_K)$: Motivated by reverse-mode differentiation [23], we use a recursive way to calculate gradients. For ease of reference, let $d\theta_t$ and dv_t denote $\frac{\partial}{\partial \theta_t} M(D_{\text{valid}}; \theta_K)$ and $\frac{\partial}{\partial v_t} M(D_{\text{valid}}; \theta_K)$ respectively. According to the chain rule to compute derivative, for any $t \in \{0, 1, 2, \dots, K-1\}$, we have

$$\begin{aligned} d\theta_t &= \left(\frac{\partial \theta_{t+1}}{\partial \theta_t}\right)^\top d\theta_{t+1} + \left(\frac{\partial v_{t+1}}{\partial \theta_t}\right)^\top dv_{t+1} = d\theta_{t+1} + \frac{\partial^2}{\partial \theta_t^2} \left[\frac{1}{|D_t|} w_t^\top \ell(D_t; \theta_t) + \lambda R(\theta_t) \right] dv_{t+1}; \\ dv_t &= \left(\frac{\partial \theta_t}{\partial v_t}\right)^\top d\theta_t + \left(\frac{\partial v_{t+1}}{\partial v_t}\right)^\top dv_{t+1} = -\eta_t d\theta_t + \mu dv_{t+1}; \\ \frac{\partial v_{t+1}}{\partial \omega} &= \frac{\partial^2}{\partial \theta_t \partial \omega} w_t^\top \ell(D_t; \theta_t); \quad \frac{\partial}{\partial \omega} M(D_{\text{valid}}; \theta_K) = \sum_{t=1}^K \left(\frac{\partial v_t}{\partial \omega}\right)^\top dv_t. \end{aligned} \quad (3)$$

According to Eqn.(3), we can design Algorithm 1 to calculate the gradients of the teacher model.

Algorithm 1: The gradients of the validation metric w.r.t. the parameters of the teacher.

- 1 *Input:* Teacher model backpropagation interval B ; parameters and momentum of the student model θ_K and v_K ; learning rates $\{\eta_t\}_{t=K-B}^{K-1}$; momentum coefficient $\mu (> 0)$; minibatches of data $\{D_t\}_{t=K-B}^{K-1}$;
 - 2 *Initialization:* $d\theta = \frac{\partial}{\partial \theta_K} M(D_{\text{valid}}; \theta_K)$; $dv = -\eta_K d\theta_K$; $d\omega \leftarrow 0$; $\theta \leftarrow \theta_K$; $v \leftarrow v_K$;
 - 3 **for** $t \leftarrow K-1 : -1 : K-B$ **do**
 - 4 $\theta \leftarrow \theta + \eta_t v$; $g \leftarrow \frac{\partial}{\partial \theta} [w_t^\top \ell(D_t; \theta) + \lambda R(\theta)]$; $v \leftarrow \frac{v-g}{\mu}$;
 - 5 $d\omega \leftarrow d\omega + \frac{\partial}{\partial \omega} (g^\top dv)$; $d\theta \leftarrow d\theta + \frac{\partial}{\partial \theta} (g^\top dv)$; $dv \leftarrow -\eta_t d\theta + \mu dv$;
 - 6 *Return* $d\omega$.
-

In Algorithm 1, we can see that we need a backpropagation interval B as an input, indicating how many internal θ 's are used to calculate the gradients of the teacher. When $B = K$, all student models on the optimization trajectory will be leveraged. B balances the tradeoff between efficiency and accuracy. To use Algorithm 1, we require $\mu > 0$.

As shown in step 2, we first calculate $\frac{\partial}{\partial \theta_K} M(D_{\text{valid}}; \theta_K)$, with which we can initialize $d\theta$, dv and $d\omega$. We then recover the θ , v and the gradients at the previous step (see step 4). Based on Eqn.(3), we recover the corresponding $d\theta$, dv and $d\omega$. We repeat step 4 and step 5 until getting the eventual $d\omega$, which is the gradient of the validation metric w.r.t. the parameters of the teacher model. Finally, we can leverage any gradient-based algorithm to update the teacher model. With the new teacher model, we can iteratively update θ^* and ω until reaching the stopping criteria.

In order to avoid calculating Hessian matrix, which needs to store $O(|\theta|^2)$ parameters, we leverage the property that $\frac{\partial^2 \ell}{\partial \theta^2} v = \frac{\partial}{\partial \theta} g^\top v$, where ℓ is the loss function related to θ , v is a vector with size $|\theta| \times 1$, and $g = \frac{\partial \ell}{\partial \theta}$. With this trick, we only require $O(|\theta|)$ GPU memory.

Discussions: Compared to previous work [14, 34, 6, 37], except for the key differences that we use internal states as features, there are some differences in optimization. In [6], the teacher is learned in a reinforcement learning manner, which is relatively hard to optimize. In [37], the student model is optimized with vanilla SGD, by which all the intermediate θ_t should be stored. In our algorithm, we use momentum SGD, where we only need to store the final θ_K and v_K , by which we can recover all intermediate parameters. We will study how to effectively apply our derivations to more optimizers and more applications in the future.

3.3 Teacher model

We introduce the default network architecture of the teacher model used in experiments. We use a linear model with sigmoid activation. Given a pair (x, y) , we first use φ_f to extract the output of the

second-to-last layer, i.e., $I = \varphi_f(x)$. The surface feature M we choose is the one-hot representation of the label, i.e., $M = y$. Then weight of the data (x, y) is $\varphi(I, M) = \sigma(W_I I + W_M E M + b)$, where $\sigma(\cdot)$ denotes the sigmoid function, W_I , W_M , E , and b are the parameters to be learned. E can be regarded as an embedding matrix, which enriches the representations of the labels. One can easily extend the teacher model to a multi-layer feed-forward network by replacing σ with a deeper network.

We need to normalize the weights within a minibatch. When a minibatch D_t comes, after calculating the weight $w_{t,k}$ for the data $(x_{t,k}, y_{t,k}) \in D_t$, it is normalized as $\tilde{w}_{t,k} = w_{t,k} / \sum_{j=1}^{|D_t|} w_{t,j}$. This is to ensure that the sum of weights within a batch D_t is always $|D_t|$.

4 Experiments on CIFAR-10/100 with clean labels

In this section, we conduct experiments on CIFAR-10 and CIFAR-100 image classification with clean labels. We first show the overall results and then provide several analysis.

4.1 Settings

There are 50000 and 10000 images in the training and test sets. CIFAR-10 and CIFAR-100 are a 10-class and a 100-class classification tasks respectively. We split 5000 samples from the training dataset as D_{valid} and the remaining 45000 samples are used as D_{train} . Following [12], we use momentum SGD with learning rate 0.1 and divide the learning rate by 10 at the 80-th and 120-th epoch. The momentum coefficient μ is 0.9. The K in B in Algorithm 1 are set as 20 and 2 respectively. We train the models for 300 epochs to ensure convergence. The minibatch size is 128. We conducted experiments on ResNet-32, ResNet-110 and Wide ResNet-28-10 (WRN-28-10) [40]. All the models are trained on a single P40 GPU.

We compare the results with the following baselines: (1) The baseline of data teaching [6] and loss function teaching [37]. They are denoted as L2T-data and L2T-loss respectively. (2) Focal loss [19], where each data is weighted by $(1 - p)^\gamma$, p is the probability that the data is correctly classified, and γ is a hyperparameter. We search γ on $\{0.5, 1, 2\}$ suggested by [19]. (3) Self-paced learning (SPL) [18], where we start from easy samples first and then move to harder examples.

4.2 Results

The test error rates of different settings are reported in Table 1. For CIFAR-10, we can see that the baseline results of ResNet-32, ResNet-110 and WRN-28-10 are 7.22, 6.38 and 4.27 respectively. With our method, we can obtain 6.20, 5.65 and 3.72 test error rates, which are the best among all listed algorithms. For CIFAR-100, our approach can improve the baseline by 0.92, 1.67 and 1.11 points. These consistent improvements demonstrate the effectiveness of our method. We have the following observations: (1) L2T-data is proposed to speed up the training. Therefore, we can see that the error rates are almost the same as the baselines. (2) For L2T-loss, on CIFAR-10 and CIFAR-100, it can achieve 0.27 and 0.32 point improvements, which are far behind of our proposed method. This shows the great advantage of our method than the previous learning to teach algorithms. (3) Focal loss sets weights to the data according to the hardness only, which does not leverage internal states neither. There exists non-negligible gap between focal loss and our method. (4) For SPL, the results are similar (even worse) to the baseline. This shows the importance of a learning based scheme for data selection.

4.3 Analysis

To further verify how our method works, we conduct several ablation studies. All experiments are conducted on CIFAR-10 with ResNet-32.

Comparison with surface information: The features of the teacher model used in Table 1 are the output of the second-to-last layer of the network (denoted as I_0), and the label embedding (denoted as M_0). Based on [34, 29, 37, 6], we define another group of features about surface information. Five components are included: the training iteration (normalized by the total number of iteration), average training loss until the current iteration, best validation accuracy until the current iteration, the predicted label of the current input, and the margin values. These surface features are denoted as M_1 .

CIFAR-10	Baseline	L2T-data [6]	L2T-loss [37]	Focal loss	SPL [18]	Ours
ResNet-32	7.22	7.16	6.95	6.60	11.48	6.20
ResNet-110	6.38	N/A	N/A	6.19	11.06	5.65
WRN-28-10	4.27	N/A	N/A	4.57	4.25	3.72
CIFAR-100	Baseline	L2T-data [6]	L2T-loss [37]	Focal loss	SPL [18]	Ours
ResNet-32	29.57	29.54	29.25	28.85	29.98	28.65
ResNet-110	27.69	N/A	N/A	26.55	27.91	26.02
WRN-28-10	20.49	N/A	N/A	19.86	20.56	19.38

Table 1: Results on CIFAR-10/CIFAR-100. The labels are clean.

For the teacher model, We try different combinations of the internal states and surface features. The settings and results are shown in Table 2.

Setting	$I_0 + M_0$	I_0	M_0	M_1	$M_0 + M_1$	$I_0 + M_0 + M_1$
Error rate	6.20	6.34	6.50	6.54	6.50	6.30

Table 2: Ablation study on the usage of features.

As shown in Table 2, we can see that the results of using surface features only (i.e., the settings without I_0) cannot catch up with those with internal states of the network (i.e., the settings with I_0). This shows the effectiveness of the internal states for learning to teach. We do not observe significant differences among the settings M_0 , M_1 and $M_0 + M_1$. Using I_0 only can result in less improvement than using $I_0 + M_0$. Combining I_0 , M_0 and M_1 also slightly hurts the result. Therefore, we choose $I_0 + M_0$ as the default setting.

Internal states from different levels: By default, we use the output of second-to-last layer as the features of internal states. We also try several other variants, naming I_1 , I_2 and I_3 , which are the outputs of the last convolutional layer with size 8×8 , 16×16 and 32×32 . A larger subscript represents that the corresponding features are more similar to the raw input. We explore the setting $I_i + M_0$, $i \in \{0, 1, 2, 3\}$. Results are reported in Table 3. We can see that leveraging internal states (i.e., I_i) can achieve lower test error rates than those without such features. Currently, there is not significant difference on where the internal states are from. Therefore, by default, we recommend to use the states from the second-to-last layer.

Setting ($I_i + M_0$)	0	1	2	3
Error rate	6.20	6.22	6.31	6.21

Table 3: Features from different levels.

Setting	MLP-0	MLP-1	MLP-2
Error rate	6.20	6.48	6.59

Table 4: Teacher with various hidden layers.

Architectures of the teacher models: We explore the teacher networks with different number of hidden layers. Each hidden layer is followed by a ReLU activation (denoted as MLP-#layer). The dimension of the hidden states are the same as the input. Results are in Table 4.

Using a more complex teacher model will not bring improvement to the simplest one as we used in the default setting. Our conjecture is that more complex models are harder to optimize, which can not provide accurate signals for the student models.

Analysis on the weights: We take comparison between the weights output by the teacher model leveraging surface features M_1 only (denoted as \mathcal{T}_0) and those output by our teacher leveraging internal features (denoted as \mathcal{T}_1). The results are shown in Figure 2, where the top row represents the results of \mathcal{T}_0 and the bottom row for \mathcal{T}_1 . In Figure 2(a), (b), (d), (e), the data points of the same category are painted with the same color. The first column shows the correlation between the output data weight (y -axis) and the training loss (x -axis); the second column is used to visualize the internal states through t-SNE [22]; the third column plots heatmaps regarding output weights of all data points (red means large weight and blue means smaller), in accordance with those in the second column. We have the following observations:

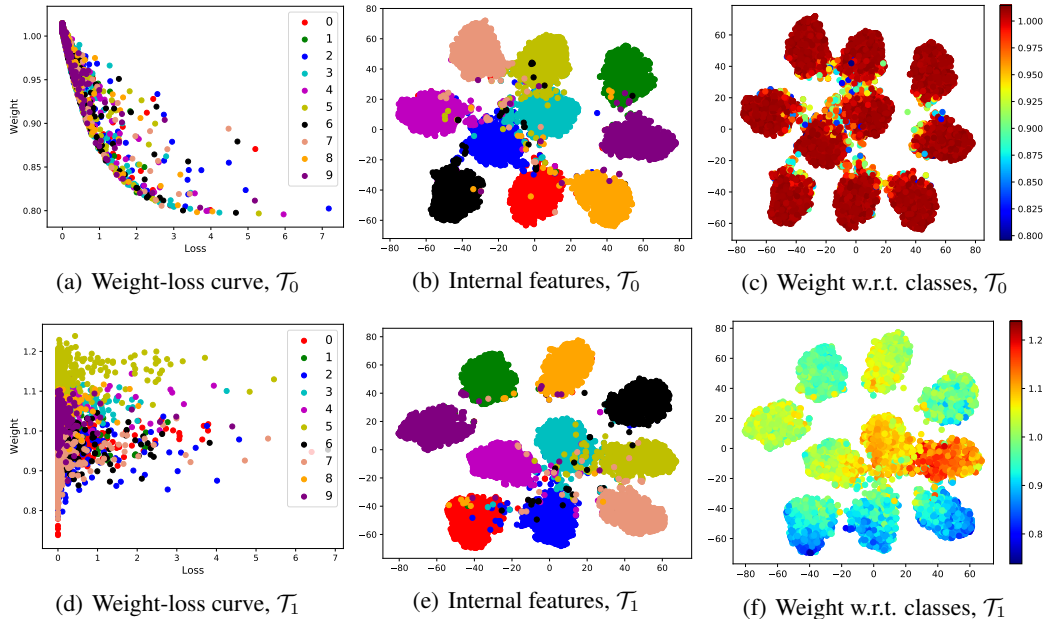


Figure 2: Visualization of weights and loss values.

(1) As shown in the first column, \mathcal{T}_0 tries to assign lower weights to the data with higher loss, regardless of the category the image belongs to. In contrast, the weights set by \mathcal{T}_1 heavily rely on the category information. For example, the data points with label 5 have the highest weights regardless of the training loss, followed by those with label 3, where label 3 and 5 correspond to the “cat” and “dog” in CIFAR-10, respectively.

(2) To further investigate the reason why the data of cat class and dog class are assigned with larger weights by \mathcal{T}_1 , we turn to Figure 2(e), from which we can find that the internal states of dog and cat are much overlapped. We therefore hypothesize that, since the dog and cat are somewhat similar to each other, \mathcal{T}_1 is learned to separate these two classes by assigning large weights to them. Yet, this phenomenon cannot be observed in \mathcal{T}_0 .

Preliminary exploration on deeper interactions: To stabilize training, we do not backpropagate the gradients to the student model via the weights, i.e., $\frac{\partial w_t}{\partial \theta_t}$ is set as zero. If we enable $\frac{\partial w_t}{\partial \theta_t}$, the teacher model will have another path to pass the supervision signal to the student model, which has great potential to improve the performances. We quickly verify this variant on CIFAR-10 using ResNet-32. We choose $I_0 + M_0$ as the features of the teacher model. We find that with this technique, we can further lower the test error rate to 6.08%, another 0.12 improvement compared to the current methods. We will further explore this direction in the future.

5 Experiments on CIFAR-10/100 with noisy labels

To verify the ability of our proposed method to deal with the noisy data, we conduct several experiments on CIFAR-10/100 datasets with noisy labels.

5.1 Settings

We derive most of the settings from [34]. The images remain the same as those in standard CIFAR-10/100, but then we introduce noise to the labels. This is to verify the effectiveness of an algorithm under the noisy setting. Two types of noise, the uniform noise and flip noise, will be introduced. For the validation and test sets, both the images and the labels are clean.

1. *Uniform noise:* We follow a common setting from [41]. The label of each image is uniformly mapped to a random class with probability p . In our experiments, we set the probability

p as 40% and 60%. Following [34], the network architecture of the student network is WRN-28-10. We use momentum SGD with learning rate 0.1 and divide the learning rate by 10 at 36-th epoch and 38-th epoch (40 epoch in total).

2. *Flip noise*: We follow [34] to set flip noise. The label of each image is independently flipped to two similar classes with probability p . The two similar classes are randomly chosen, and we flip labels to them with equal probability. In our experiments, we set probability p as 20% and 40% and adopt ResNet-32 as the student model. We use momentum SGD with learning rate 0.1 and divide the learning rate by 10 at 40-th epoch and 50-th epoch (60 epoch in total).

For the teacher model, we follow settings in Section 4. We compare the results with MentorNet [14] and Meta-Weight-Net [34].

5.2 Results

The results are shown in Table 5 and Table 6. We can see that our results are better than the previous baselines like MentorNet and Meta-Weight-Net, regardless of the type and magnitude. When the noise type is uniform, we can improve Meta-Weight-Net by about 0.5 point. On flip noise with ResNet-32 network, the improvement is more significant, where in most cases, we can improve the baseline by more than one point.

The experiment results demonstrate that leveraging internal states is also useful for the datasets with noisy labels. This shows the generality of our proposed method.

Method	CIFAR-10		CIFAR-100	
	$p = 40\%$	$p = 60\%$	$p = 40\%$	$p = 60\%$
Baseline	31.93	46.88	48.89	69.08
MentorNet [14]	12.67	17.20	38.61	63.13
Meta-Weight-Net [34]	10.73	15.93	32.27	41.25
Ours	10.29	15.37	31.36	40.62

Table 5: Results of WRN-28-10 on uniform noise label CIFAR-10/100 datasets.

Method	CIFAR-10		CIFAR-100	
	$p = 20\%$	$p = 40\%$	$p = 20\%$	$p = 40\%$
Baseline	23.17	29.23	49.14	56.99
MentorNet [14]	13.64	18.24	38.03	47.34
Meta-Weight-Net [34]	9.67	12.46	35.78	41.36
Ours	8.95	11.29	33.92	39.49

Table 6: Results of ResNet-32 on flip noise label CIFAR-10/100 datasets.

6 Conclusion and future work

We propose a new data teaching paradigm, where the teacher and student model have deep interactions. The internal states are fed into the teacher model to calculate the weights of the data, and we propose an algorithm to jointly optimize the two models. Experiments on CIFAR-10 and CIFAR-100 with clean and noisy labels demonstrate the effectiveness of our approach. Rich ablation studies are conducted in this work.

For future work, the first one is to study how to apply deeper interaction to the learning to teach framework (preliminary results in Section 4.3). Second, we want that the teacher model could be transferred across different tasks, which is lacked for the current teacher (see Appendix B for the exploration). Third, we will carry out theoretical analysis on the convergence of the optimization algorithm.

Appendix

A Ablation study on different K and B

In this section, we conduct an ablation study to explore the impact of different model update interval K and backpropagation interval B on our algorithm. We adopt CIFAR-10 and ResNet-32 as the base dataset and student model respectively. We choose $(K, B) \in \{(1, 1), (20, 2), (20, 5), (100, 2), (100, 5)\}$ in our ablation study. In Table 1 in the main paper, we use $K = 20$ and $B = 2$ as the default setting.

K	B	Test error
1	1	6.56
20	2	6.20
20	5	6.41
100	2	6.30
100	5	6.24

Table 7: Error rates of different K and B on CIFAR-10 and student model ResNet-32.

The ablation study results are reported in Table 7. We can observe that 1) The setting that run backpropagation at each step ($K = 1, B = 1$) takes high computational cost and is hard to optimize the teacher model. 2) Our default setting can reach the lowest test error rate among all (K, B) settings.

B Transferability of the teacher across different tasks

In this section, we conduct some experiments to explore the transferability of our teacher models across different tasks.

We choose our best setting 6.20 (the dataset is CIFAR-10, and the architecture of the student model is ResNet-32) in Table 1 as the original teacher model, and adopt two transfer settings.

(1) *Transfer to different dataset*: We transfer our original teacher model from CIFAR-10 to CIFAR-100 dataset. The network architecture of the student model remains unchanged.

(2) *Transfer to different student model*: We change the student model architecture from ResNet-32 to ResNet-110. The dataset remains unchanged.

In the above two settings, we train the student models from scratch and fix the parameters of the teacher models. The teacher models provide weights for the input data.

The test error rates of *Transfer to different dataset* and *Transfer to different student model* are 92.45% and 57.97% respectively. Our teacher models lack transferability due to deep interactions between the teacher and the student models. We will improve our algorithm to enhance the transferability in future.

References

- [1] Gustavo Aguilar, Yuan Ling, Yu Zhang, Benjamin Yao, Xing Fan, and Edward Guo. Knowledge distillation from internal representations. *AAAI*, 2020.
- [2] Peter Anderson, Xiaodong He, Chris Buehler, Damien Teney, Mark Johnson, Stephen Gould, and Lei Zhang. Bottom-up and top-down attention for image captioning and visual question answering. In *Proceedings of the IEEE conference on computer vision and pattern recognition*, pages 6077–6086, 2018.
- [3] Dana Angluin and Philip Laird. Learning from noisy examples. *Machine Learning*, 2(4):343–370, 1988.
- [4] Yoshua Bengio, Jérôme Louradour, Ronan Collobert, and Jason Weston. Curriculum learning. In *Proceedings of the 26th annual international conference on machine learning*, pages 41–48, 2009.

- [5] Qi Dong, Shaogang Gong, and Xiatian Zhu. Class rectification hard mining for imbalanced deep learning. In *Proceedings of the IEEE International Conference on Computer Vision*, pages 1851–1860, 2017.
- [6] Yang Fan, Fei Tian, Tao Qin, Xiang-Yang Li, and Tie-Yan Liu. Learning to teach. In *Sixth International Conference on Learning Representations*, 2018.
- [7] Y Freund and R Shapire. A decision-theoretic generalization of on-line learning and an application to boosting. *J Comput Syst Sci*, 55:119–139, 1997.
- [8] Jerome Friedman, Trevor Hastie, Robert Tibshirani, et al. Additive logistic regression: a statistical view of boosting (with discussion and a rejoinder by the authors). *The annals of statistics*, 28(2):337–407, 2000.
- [9] Chen Gong, Dacheng Tao, Wei Liu, Liu Liu, and Jie Yang. Label propagation via teaching-to-learn and learning-to-teach. *IEEE transactions on neural networks and learning systems*, 28(6):1452–1465, 2016.
- [10] Chen Gong, Dacheng Tao, Jie Yang, and Wei Liu. Teaching-to-learn and learning-to-teach for multi-label propagation. In *Thirtieth AAAI conference on artificial intelligence*, 2016.
- [11] Trevor Hastie, Saharon Rosset, Ji Zhu, and Hui Zou. Multi-class adaboost. *Statistics and its Interface*, 2(3):349–360, 2009.
- [12] K. He, X. Zhang, S. Ren, and J. Sun. Deep residual learning for image recognition. In *2016 IEEE Conference on Computer Vision and Pattern Recognition (CVPR)*, pages 770–778, 2016.
- [13] Mark K Ho, Michael Littman, James MacGlashan, Fiery Cushman, and Joseph L Austerweil. Showing versus doing: Teaching by demonstration. In *Advances in neural information processing systems*, pages 3027–3035, 2016.
- [14] Lu Jiang, Zhengyuan Zhou, Thomas Leung, Li-Jia Li, and Li Fei-Fei. Mentornet: Learning data-driven curriculum for very deep neural networks on corrupted labels. In *Thirty-fifth International Conference on Machine Learning*, 2018.
- [15] S. H. Khan, M. Hayat, M. Bennamoun, F. A. Sohel, and R. Togneri. Cost-sensitive learning of deep feature representations from imbalanced data. *IEEE Transactions on Neural Networks and Learning Systems*, 29(8):3573–3587, 2018.
- [16] Pang Wei Koh and Percy Liang. Understanding black-box predictions via influence functions. In *Proceedings of the 34th International Conference on Machine Learning-Volume 70*, pages 1885–1894. JMLR. org, 2017.
- [17] Alex Krizhevsky, Geoffrey Hinton, et al. Learning multiple layers of features from tiny images. 2009.
- [18] M. P. Kumar, Benjamin Packer, and Daphne Koller. Self-paced learning for latent variable models. In J. D. Lafferty, C. K. I. Williams, J. Shawe-Taylor, R. S. Zemel, and A. Culotta, editors, *Advances in Neural Information Processing Systems 23*, pages 1189–1197. Curran Associates, Inc., 2010.
- [19] Tsung-Yi Lin, Priya Goyal, Ross Girshick, Kaiming He, and Piotr Dollár. Focal loss for dense object detection. In *Proceedings of the IEEE international conference on computer vision*, pages 2980–2988, 2017.
- [20] Ji Liu and Xiaojin Zhu. The teaching dimension of linear learners. *Journal of Machine Learning Research*, 17(162):1–25, 2016.
- [21] Weiyang Liu, Bo Dai, Ahmad Humayun, Charlene Tay, Chen Yu, Linda B Smith, James M Rehg, and Le Song. Iterative machine teaching. In *Proceedings of the 34th International Conference on Machine Learning-Volume 70*, pages 2149–2158. JMLR. org, 2017.
- [22] Laurens van der Maaten and Geoffrey Hinton. Visualizing data using t-sne. *Journal of machine learning research*, 9(Nov):2579–2605, 2008.
- [23] Dougal Maclaurin, David Duvenaud, and Ryan Adams. Gradient-based hyperparameter optimization through reversible learning. In *International Conference on Machine Learning*, pages 2113–2122, 2015.
- [24] Tomasz Malisiewicz, Abhinav Gupta, and Alexei A Efros. Ensemble of exemplar-svms for object detection and beyond. In *2011 International conference on computer vision*, pages 89–96. IEEE, 2011.

- [25] Adam Paszke, Sam Gross, Francisco Massa, Adam Lerer, James Bradbury, Gregory Chanan, Trevor Killeen, Zeming Lin, Natalia Gimelshein, Luca Antiga, Alban Desmaison, Andreas Kopf, Edward Yang, Zachary DeVito, Martin Raison, Alykhan Tejani, Sasank Chilamkurthy, Benoit Steiner, Lu Fang, Junjie Bai, and Soumith Chintala. Pytorch: An imperative style, high-performance deep learning library. In *Advances in Neural Information Processing Systems* 32, pages 8024–8035. 2019.
- [26] Matthew Peters, Mark Neumann, Mohit Iyyer, Matt Gardner, Christopher Clark, Kenton Lee, and Luke Zettlemoyer. Deep contextualized word representations. In *Proceedings of the 2018 Conference of the North American Chapter of the Association for Computational Linguistics: Human Language Technologies, Volume 1 (Long Papers)*, pages 2227–2237, New Orleans, Louisiana, June 2018. Association for Computational Linguistics.
- [27] Boris T Polyak. Some methods of speeding up the convergence of iteration methods. *USSR Computational Mathematics and Mathematical Physics*, 4(5):1–17, 1964.
- [28] Scott Reed, Honglak Lee, Dragomir Anguelov, Christian Szegedy, Dumitru Erhan, and Andrew Rabinovich. Training deep neural networks on noisy labels with bootstrapping. *arXiv preprint arXiv:1412.6596*, 2014.
- [29] Mengye Ren, Wenyuan Zeng, Bin Yang, and Raquel Urtasun. Learning to reweight examples for robust deep learning. In *Thirty-fifth International Conference on Machine Learning*, 2018.
- [30] Shaoqing Ren, Kaiming He, Ross Girshick, and Jian Sun. Faster r-cnn: Towards real-time object detection with region proposal networks. In C. Cortes, N. D. Lawrence, D. D. Lee, M. Sugiyama, and R. Garnett, editors, *Advances in Neural Information Processing Systems 28*, pages 91–99. Curran Associates, Inc., 2015.
- [31] Adriana Romero, Nicolas Ballas, Samira Ebrahimi Kahou, Antoine Chassang, Carlo Gatta, and Yoshua Bengio. Fitnets: Hints for thin deep nets. *ICLR*, 2015.
- [32] Robert E Schapire, Yoav Freund, Peter Bartlett, Wee Sun Lee, et al. Boosting the margin: A new explanation for the effectiveness of voting methods. *The annals of statistics*, 26(5):1651–1686, 1998.
- [33] Patrick Shafto, Noah D Goodman, and Thomas L Griffiths. A rational account of pedagogical reasoning: Teaching by, and learning from, examples. *Cognitive psychology*, 71:55–89, 2014.
- [34] Jun Shu, Qi Xie, Lixuan Yi, Qian Zhao, Sanping Zhou, Zongben Xu, and Deyu Meng. Meta-weight-net: Learning an explicit mapping for sample weighting. In *Advances in Neural Information Processing Systems 32*, pages 1919–1930. Curran Associates, Inc., 2019.
- [35] Sainbayar Sukhbaatar and Rob Fergus. Learning from noisy labels with deep neural networks. *arXiv preprint arXiv:1406.2080*, 2(3):4, 2014.
- [36] Yanmin Sun, Mohamed S. Kamel, Andrew K.C. Wong, and Yang Wang. Cost-sensitive boosting for classification of imbalanced data. *Pattern Recognition*, 40(12):3358 – 3378, 2007.
- [37] Lijun Wu, Fei Tian, Yingce Xia, Yang Fan, Tao Qin, Lai Jian-Huang, and Tie-Yan Liu. Learning to teach with dynamic loss functions. In *Advances in Neural Information Processing Systems 31*, pages 6466–6477, 2018.
- [38] Kelvin Xu, Jimmy Ba, Ryan Kiros, Kyunghyun Cho, Aaron Courville, Ruslan Salakhudinov, Rich Zemel, and Yoshua Bengio. Show, attend and tell: Neural image caption generation with visual attention. In *International conference on machine learning*, pages 2048–2057, 2015.
- [39] Bianca Zadrozny. Learning and evaluating classifiers under sample selection bias. In *Proceedings of the twenty-first international conference on Machine learning*, page 114, 2004.
- [40] Sergey Zagoruyko and Nikos Komodakis. Wide residual networks. In Edwin R. Hancock Richard C. Wilson and William A. P. Smith, editors, *Proceedings of the British Machine Vision Conference (BMVC)*, pages 87.1–87.12. BMVA Press, September 2016.
- [41] Chiyuan Zhang, Samy Bengio, Moritz Hardt, Benjamin Recht, and Oriol Vinyals. Understanding deep learning requires rethinking generalization. In *5th International Conference on Learning Representations, ICLR 2017, Toulon, France, April 24-26, 2017, Conference Track Proceedings*. OpenReview.net, 2017.
- [42] Xiaojin Zhu. Machine teaching: An inverse problem to machine learning and an approach toward optimal education. In *Twenty-Ninth AAAI Conference on Artificial Intelligence*, 2015.